Journal of Nonlinear Dynamics and Applications
http://dx.doi.org/10.62762/JNDA.2025.473008

RESEARCH ARTICLE

Further Analysis on Preassigned-time Anti-synchronization of Memristive Inertial BAM Neural Networks

Xiao Zhou[1,*], **Jingrui Hou**[2] **and Guodong Zhang**[1]

[1] School of Mathematics and Statistics, South-Central Minzu University, Wuhan 430074, China
[2] School of Engineering, RMIT University, Melbourne, VIC 3001, Australia

Abstract

This paper studies the preassigned time anti-synchronization control problem of a class of bidirectional associative memory (BAM) neural networks with inertia terms and memristor characteristics. By constructing a novel Lyapunov-Krasovskii function and combining it with the latest fixed-time stability theory, it strictly proves the sufficient conditions for the system to achieve anti-synchronization within the preassigned time. Numerical simulations further verified the effectiveness and superiority of the method, especially demonstrating higher accuracy and flexibility when dealing with high-order dynamics and memristor-based systems.

Keywords: preassigned-time anti-synchronization, non-reduced method, mixed delays, memristive inertial BAM neural networks.

1 Introduction

In recent years, bidirectional associative memory (BAM) neural networks [1–3] have shown broad application prospects in fields such as pattern recognition, intelligent control, and information security due to their unique bidirectional information processing capabilities and associative memory characteristics [4, 5]. Especially when inertia terms [6] and memristors [7] are introduced, such networks can be used to simulate the dynamic behavior of biological neurons and the plasticity of synapses. The inertia term reflects the dynamic lag effect of neurons, while the memristor endows the network with non-volatile memory characteristics. The combination of the two makes the system's dynamic behavior more complex and closer to that of a real biological nervous system. In recent years, there have been many papers on BAM neural networks here [8–11].

Before delving into system control issues, it is necessary to first understand the characteristics of the key component, the memristor. The resistance value of a memristor depends on the amount of charge or magnetic flux passing through it and can simulate the non-volatile memory and nonlinear dynamic behavior of biological synapses [14]. Introducing memristors into neural networks not only enables more efficient hardware implementation (such as neuromorphic chips), but also endows the system with adaptability and historical dependence, thereby significantly enhancing the network's information processing capabilities [15]. However, the multi-valued characteristics and switching nonlinearity of memristors also bring new theoretical

Submitted: 13 August 2025
Accepted: 17 September 2025
Published: 19 November 2025

Vol. 1, **No.** 2, 2025.
10.62762/JNDA.2025.473008

***Corresponding author:**
Xiao Zhou
zx187270@163.com

Citation
Zhou, X., Hou, J., & Zhang, G. (2025). Further Analysis on Preassigned-time Anti-synchronization of Memristive Inertial BAM Neural Networks. *Journal of Nonlinear Dynamics and Applications*, 1(2), 63–75.

challenges: on the one hand, their continuous or discrete resistive state switching can lead to the system dynamically presenting piecewise smooth or even discontinuous characteristics. On the other hand, the time-varying characteristics of the memristor [16] coupling term make traditional stability analysis methods (such as the theory based on Lipschitz continuity) difficult to be directly applied. Especially in the problem of preset time control, the coupling of the memristor state and the inertia term further increases the complexity of controller design, and there is an urgent need to develop new analytical tools to precisely characterize the transient behavior of the system.

In the face of these challenges, traditional solutions often have obvious deficiencies. Specifically, most of the traditional research on synchronous control of discontinuous inertial neural networks adopts the order reduction method, that is, by replacing state variables, the second-order discontinuous differential equation is transformed into a system of first-order equations [17–20]. Although this method simplifies theoretical analysis, it also brings obvious limitations: Firstly, the order reduction process introduces additional state variables, leading to the expansion of system dimensions and increasing computational complexity; Secondly, the split equations often fail to fully retain the physical meaning and dynamic characteristics of the original system. More importantly, the stability conditions derived from this are usually rather conservative and difficult to achieve precise time control. In addition, existing research mainly focuses on asymptotic synchronization [21–23] or finite-time synchronization [9, 24–27], whose convergence time depends on the initial state of the system and cannot meet the strict requirements of the preset time (i.e., users can specify the convergence time in advance) in actual engineering. These flaws severely limit the application of such methods in high-precision control scenarios.

Based on the above analysis, Preassigned time anti-synchronization is a cutting-edge research direction in the field of neural network control. Its core goal is to design a controller to precisely achieve anti-synchronization of the system state within the time preset by the user. And the convergence time is completely independent of the initial state. This feature has key application value in scenarios with extremely high time sensitivity requirements such as secure communication and fault detection. Compared with traditional asymptotic synchronization or finite-time synchronization, preassigned time synchronization [28–31] offers stricter time controllability: system errors can converge to zero at the exact moment specified by engineering requirements, rather than relying solely on initial conditions or system parameters. The neural networks studied in [12, 13, 30, 32] did not take memristors into account, but this paper studies them. Unlike [33] which studies the anti-synchronization problem of BAM neural networks, we are researching the anti-synchronization [32–34] problem of inertial BAM neural networks. From the above, it can be known that the neural network studied in this paper is more comprehensive, However, there are few related papers that study the preassigned time anti-synchronization (PTAS) of inertial memristor BAM neural networks (BAM-IMNNS) using non-reduced-order methods. The research in this paper can fill this gap.

Be insptred by the above, our article aims to research the PTAS issues for BAM-IMNNs. And the innovations of our article are presented below:

(1)The research system of this paper includes the inertia term, the memristor term, and BAM. However, there are relatively few results related to the inertia term and memristors with BAM neural networks. Our research content can fill this gap and provide a theoretical basis for related studies.

(2)Different from many results on synchronization of discontinuous inertial neural networks, the variable separation method they used lacked of preciseness, we can effectively avoid these problems by using the non-reduced to discuss the problem of BAM-IMNNs.

(3)This paper studies the preassigned time anti-synchronization problem of the system, which can precisely achieve anti-synchronization within the preset time, and the convergence time is completely independent of the initial state.

The work arrangement of our research is as follows: Part 2, preliminaries are illustrated. Part 3, PTAS standards of BAM-IMNNs are given. Part 4, simulations are displayed. Lastly, conclusions are showed.

Notations: Let $\mathfrak{D} = \Big\{1, 2, ...k_1\Big\}$, $\Re = \Big\{1, 2, ...k_2\Big\}$, $\Im = \Big\{0, 1, 2, ...\Big\}$, $\mathbf{R}^k$ is k-dimensional Euclidean space. And for $\forall z = (z_1, z_2, ...z_k)^T \in \mathbf{R}^k$, $||z|| = \sum_{i=1}^{k} |z_i|$, $co[\Omega]$ is the convex closure of set Ω. $D^+V(t)$ is Dini derivative with top right of $V(t)$ that is continuous function. Let $\S = max\Big\{\tau, \eta\Big\}$,

$\mathcal{C}([-\S,0],\mathbf{R}^{k_1})$ demonstrates all continuous-functions from $[-\S,0]$ into $\mathbf{R}^{k_1}$ and $\S^* = max\Big\{\sigma,\iota\Big\}$, $\mathcal{C}([-\S^*,0],\mathbf{R}^{k_2})$ demonstrates all continuous-functions from $[-\S^*,0]$ into $\mathbf{R}^{k_2}$. $A_{\omega\varsigma} = max\Big\{|a^+_{\omega\varsigma}|,|a^-_{\omega\varsigma}|\Big\}$, $B_{\omega\varsigma} = max\Big\{|b^+_{\omega\varsigma}|,|b^-_{\omega\varsigma}|\Big\}$,$\theta = max\Big\{|\theta^+_{\omega\varsigma}|,|\theta^-_{\omega\varsigma}|\Big\}$, $\beta_\varsigma = min\Big\{|\beta^+_\varsigma|,|\beta^-_\varsigma|\Big\}$, $C_{\varsigma\omega} = max\Big\{|c^+_{\varsigma\omega}|,|c^-_{\varsigma\omega}|\Big\}$, $D_{\varsigma\omega} = max\Big\{|d^+_{\varsigma\omega}|,|d^-_{\varsigma\omega}|\Big\}$,$\vartheta = max\Big\{|\vartheta^+_{\varsigma\omega}|,|\vartheta^-_{\varsigma\omega}|\Big\}$.

2 Preliminaries

2.1 Model and Assumptions

The BAM-IMNNs is

$$\begin{aligned}
\frac{\mathrm{d}^2x_\omega(t)}{\mathrm{d}t^2} =& -\lambda_\omega x_\omega(t) - \mu_\omega\frac{\mathrm{d}x_\omega(t)}{\mathrm{d}t} + \sum_{\varsigma=1}^{k_2} a_{\omega\varsigma}(x_\omega(t)) \\
&\times f_\varsigma(y_\varsigma(t)) + \sum_{\varsigma=1}^{k_2} b_{\omega\varsigma}(x_\omega(t)) f_\varsigma(y_\varsigma(t-\tau(t))) \\
&+ \sum_{\varsigma=1}^{k_2}\theta_{\omega\varsigma}(x_\omega(t))\int_{t-\eta(t)}^{t} f_\varsigma(y_\varsigma(s))\mathrm{d}s + \Gamma_\omega, \\
\frac{\mathrm{d}^2y_\varsigma(t)}{\mathrm{d}t^2} =& -\alpha_\varsigma y_\varsigma(t) - \beta_\varsigma\frac{\mathrm{d}y_\varsigma(t)}{\mathrm{d}t} + \sum_{\omega=1}^{k_1} c_{\varsigma\omega}(y_\varsigma(t)) \\
&\times g_\omega(x_\omega(t)) + \sum_{\omega=1}^{k_1} d_{\varsigma\omega}(y_\varsigma(t)) g_\omega(x_\omega(t-\sigma(t))) \\
&+ \sum_{\omega=1}^{k_1}\vartheta_{\varsigma\omega}(y_\varsigma(t))\int_{t-\iota(t)}^{t} g_\omega(x_\omega(s))\mathrm{d}s + \Upsilon_\varsigma, \\
&\omega\in\mathfrak{D}, \varsigma\in\mathfrak{R}, t\geq 0, \qquad (1)
\end{aligned}$$

where

$$a_{\omega\varsigma}(x_\omega(t)) = \begin{cases} a^+_{\omega\varsigma}, \phi_{\omega\varsigma}\frac{\mathrm{d}f_\varsigma(x_\varsigma(t))}{\mathrm{d}t} \leq \frac{\mathrm{d}x_\omega(t)}{\mathrm{d}t} \\ a^-_{\omega\varsigma}, \phi_{\omega\varsigma}\frac{\mathrm{d}f_\varsigma(x_\varsigma(t))}{\mathrm{d}t} > \frac{\mathrm{d}x_\omega(t)}{\mathrm{d}t} \end{cases}$$

$$b_{\omega\varsigma}(x_\omega(t)) = \begin{cases} b^+_{\omega\varsigma}, \phi_{\omega\varsigma}\frac{\mathrm{d}f_\varsigma(x_\varsigma(t-\tau(t)))}{\mathrm{d}t} \leq \frac{\mathrm{d}x_\omega(t)}{\mathrm{d}t} \\ b^-_{\omega\varsigma}, \phi_{\omega\varsigma}\frac{\mathrm{d}f_\varsigma(x_\varsigma(t-\tau(t)))}{\mathrm{d}t} > \frac{\mathrm{d}x_\omega(t)}{\mathrm{d}t} \end{cases}$$

$$\theta_{\omega\varsigma}(x_\omega(t)) = \begin{cases} \theta^+_{\omega\varsigma}, \phi_{\omega\varsigma}\frac{\mathrm{d}\int_{t-\eta(t)}^{t} f_\varsigma(x_\varsigma(s))ds}{\mathrm{d}t} \leq \frac{\mathrm{d}x_\omega(t)}{\mathrm{d}t} \\ \theta^-_{\omega\varsigma}, \phi_{\omega\varsigma}\frac{\mathrm{d}\int_{t-\eta(t)}^{t} f_\varsigma(x_\varsigma(s))ds}{\mathrm{d}t} > \frac{\mathrm{d}x_\omega(t)}{\mathrm{d}t} \end{cases} \qquad (2)$$

$$c_{\varsigma\omega}(y_\varsigma(t)) = \begin{cases} c^+_{\varsigma\omega}, \phi_{\varsigma\omega}\frac{\mathrm{d}g_\omega(y_\omega(t))}{\mathrm{d}t} \leq \frac{\mathrm{d}y_\varsigma(t)}{\mathrm{d}t} \\ c^-_{\varsigma\omega}, \phi_{\varsigma\omega}\frac{\mathrm{d}g_\omega(y_\omega(t))}{\mathrm{d}t} > \frac{\mathrm{d}y_\varsigma(t)}{\mathrm{d}t} \end{cases}$$

$$d_{\varsigma\omega}(y_\varsigma(t)) = \begin{cases} d^+_{\varsigma\omega}, \phi_{\varsigma\omega}\frac{\mathrm{d}g_\omega(y_\omega(t-\sigma(t)))}{\mathrm{d}t} \leq \frac{\mathrm{d}y_\varsigma(t)}{\mathrm{d}t} \\ d^-_{\varsigma\omega}, \phi_{\varsigma\omega}\frac{\mathrm{d}g_\omega(y_\omega(t-\sigma(t)))}{\mathrm{d}t} > \frac{\mathrm{d}y_\varsigma(t)}{\mathrm{d}t} \end{cases}$$

$$\vartheta_{\varsigma\omega}(y_\varsigma(t)) = \begin{cases} \vartheta^+_{\varsigma\omega}, \phi_{\varsigma\omega}\frac{\mathrm{d}\int_{t-\iota(t)}^{t} g_\omega(y_\omega(s))ds}{\mathrm{d}t} \leq \frac{\mathrm{d}y_\varsigma(t)}{\mathrm{d}t} \\ \vartheta^-_{\varsigma\omega}, \phi_{\varsigma\omega}\frac{\mathrm{d}\int_{t-\iota(t)}^{t} g_\omega(y_\omega(s))ds}{\mathrm{d}t} > \frac{\mathrm{d}y_\varsigma(t)}{\mathrm{d}t} \end{cases} \qquad (3)$$

where $\phi_{\omega\varsigma} = \phi_{\varsigma\omega} = 1(\omega\neq\varsigma)$, if not, -1. $\Gamma_\omega,\Upsilon_\varsigma$ are external input, And $\lambda_\omega,\mu_\omega,\alpha_\varsigma,\beta_\varsigma > 0$, other connection weights $a^+_{\omega\varsigma},a^-_{\omega\varsigma},b^+_{\omega\varsigma},b^-_{\omega\varsigma}$, $\theta^+_{\omega\varsigma},\theta^-_{\omega\varsigma},c^+_{\varsigma\omega},c^-_{\varsigma\omega},d^+_{\varsigma\omega},d^-_{\varsigma\omega},\vartheta^+_{\varsigma\omega},\vartheta^-_{\varsigma\omega}$ are all constants. $g_\omega(\cdot),f_\varsigma(\cdot)$ is feedback function. Time-delays $\tau(t)$,$\eta(t)$,σ_ς,$\iota_\varsigma$and $0<\tau(t)\leqslant\tau$, $0<\eta(t)\leqslant\eta$,$0<\sigma(t)\leqslant\sigma$, $0<\iota(t)\leqslant\iota$ respectively. The initial data of BAM-IMNNs (1) are prescribed as $x_\omega(\ddagger) = \chi_\omega(\ddagger),\dot{x}_\omega(\ddagger) = \varphi_\omega(\ddagger)$,$y_\varsigma(\ddagger) = \tilde{\chi}_\varsigma(\ddagger),\dot{y}_\varsigma(\ddagger) = \tilde{\varphi}_\varsigma(\ddagger)$ and $\chi_\omega(\ddagger),\varphi_\omega(\ddagger)\in\mathcal{C}([-\S,0],\mathbf{R}),\ddagger\in[-\S,0]$, $\tilde{\chi}_\varsigma(\ddagger),\tilde{\varphi}_\varsigma(\ddagger)\in\mathcal{C}([-\S^*,0],\mathbf{R}),\ddagger\in[-\S^*,0]$, $\omega\in\mathfrak{D},\varsigma\in\mathfrak{R}$.

Assumption1: The activation function satisfies $|g_\omega(\cdot)|\leqslant\Pi_\omega$, $\Pi_\omega>0$, $|f_\varsigma(\cdot)|\leqslant\Pi_\varsigma$, $\Pi_\varsigma>0$.

2.2 Difinition of Filippov solution

Owing to switched-connection (2) and (3), BAM-IMNNs (1) is discontinuous. By using theory of differential inclusions theories [35] and from (1), one get

$$\begin{aligned}
&\frac{\mathrm{d}^2x_w(t)}{\mathrm{d}t^2} + \mu_\omega\frac{\mathrm{d}x_\omega(t)}{\mathrm{d}t} \in -\lambda_\omega x_\omega(t) + \sum_{\varsigma=1}^{k_2} co[a_{\omega\varsigma}(x_\omega(t))] \\
&f_\varsigma(y_\varsigma(t)) + \sum_{\varsigma=1}^{k_2} co[b_{\omega\varsigma}(x_\omega(t))] f_\varsigma(y_\varsigma(t-\tau(t))) \\
&+ \sum_{\varsigma=1}^{k_2} co[\theta_{\omega\varsigma}(x_\omega(t))]\int_{t-\eta(t)}^{t} f_\varsigma(y_\varsigma(s))\mathrm{d}s + \Gamma_\omega, \\
&\frac{\mathrm{d}^2y_\varsigma(t)}{\mathrm{d}t^2} + \beta_\varsigma\frac{\mathrm{d}y_\varsigma(t)}{\mathrm{d}t} \in -\alpha_\varsigma y_\varsigma(t) + \sum_{\omega=1}^{k_1} co[c_{\varsigma\omega}(y_\varsigma(t))] \\
&g_\omega(x_\omega(t)) + \sum_{\omega=1}^{k_1} co[d_{\varsigma\omega}(y_\varsigma(t))] g_\omega(x_\omega(t-\sigma(t))) \\
&+ \sum_{\omega=1}^{k_1} co[\vartheta_{\varsigma\omega}(y_\varsigma(t))]\int_{t-\iota(t)}^{t} g_\omega(x_\omega(s))\mathrm{d}s + \Upsilon_\varsigma, \\
&\omega\in\mathfrak{D}, \varsigma\in\mathfrak{R}, t\geq 0, \qquad (4)
\end{aligned}$$

equivalent

$$
\begin{aligned}
&\frac{\mathrm{d}^2 x_\omega(t)}{\mathrm{d}t^2} + \mu_\omega \frac{\mathrm{d}x_\omega(t)}{\mathrm{d}t} = -\lambda_\omega x_\omega(t) + \sum_{\varsigma=1}^{k_2} a_{\omega\varsigma}(t) \\
&\times f_\varsigma(y_\varsigma(t)) + \sum_{\varsigma=1}^{k_2} b_{\omega\varsigma}(t) f_\varsigma(y_\varsigma(t-\tau(t))) \\
&+ \sum_{\varsigma=1}^{k_2} \theta_{\omega\varsigma}(t) \int_{t-\eta(t)}^{t} f_\varsigma(y_\varsigma(s))\mathrm{d}s + \Gamma_\omega, \\
&\frac{\mathrm{d}^2 y_\varsigma(t)}{\mathrm{d}t^2} + \beta_\varsigma \frac{\mathrm{d}y_\varsigma(t)}{\mathrm{d}t} = -\alpha_\varsigma y_\varsigma(t) + \sum_{\omega=1}^{k_1} c_{\varsigma\omega}(t) \\
&\times g_\omega(x_\omega(t)) + \sum_{\omega=1}^{k_1} d_{\varsigma\omega}(t) g_\omega(x_\omega(t-\sigma(t))) \\
&+ \sum_{\omega=1}^{k_1} \vartheta_{\varsigma\omega}(t) \int_{t-\iota(t)}^{t} g_\omega(x_\omega(s))\mathrm{d}s + \Upsilon_\varsigma, \\
&\omega \in \mathfrak{D}, \varsigma \in \Re, t \geq 0, \qquad (5)
\end{aligned}
$$

where $a_{\omega\varsigma}(t) \in co[a_{\omega\varsigma}(x_\omega(t))]$, $b_{\omega\varsigma}(t) \in co[b_{\omega\varsigma}(x_\omega(t))]$, $\theta_{\omega\varsigma}(t) \in co[\theta_{\omega\varsigma}(x_\omega(t))]$, $c_{\varsigma\omega}(t) \in co[c_{\varsigma\omega}(y_\varsigma(t))]$, $d_{\varsigma\omega}(t) \in co[d_{\varsigma\omega}(y_\varsigma(t))]$, $\vartheta_{\varsigma\omega}(t) \in co[\vartheta_{\varsigma\omega}(y_\varsigma(t))]$.

Definition 1 ([36]). The function $x(t) = (x_1(t), x_2(t), ...x_{k_1}(t))^T$, $y(t) = (y_1(t), y_2(t), ...y_{k_2}(t))^T$ is a Filippov-solution of BAM-IMNNs (1) with initial position $x_\omega(\ddagger) = \chi_\omega(\ddagger), \dot{x}_\omega(\ddagger) = \varphi_\omega(\ddagger)$,$y_\varsigma(\ddagger) = \tilde{\chi}_\varsigma(\ddagger), \dot{y}_\varsigma(\ddagger) = \tilde{\varphi}_\varsigma(\ddagger)$ and $\chi_\omega(\ddagger), \varphi_\omega(\ddagger) \in \mathcal{C}([-\S, 0], \mathbf{R}), \ddagger \in [-\S, 0]$, $\tilde{\chi}_\varsigma(\ddagger), \tilde{\varphi}_\varsigma(\ddagger) \in \mathcal{C}([-\S^*, 0], \mathbf{R}), \ddagger \in [-\S^*, 0], \omega \in \mathfrak{D}, \varsigma \in \Re$. For all compact-interval of $[0, +\infty)$, the function $x(t)$, $y(t)$ meets system (4) and (5).

2.3 Error model between BAM-IMNNs (1) and (7)

Now, we take corresponding response-model of BAM-IMNNs (1) below:

$$
\begin{aligned}
\frac{\mathrm{d}^2 p_\omega(t)}{\mathrm{d}t^2} =& - \lambda_\omega p_\omega(t) - \mu_\omega \frac{\mathrm{d}p_\omega(t)}{\mathrm{d}t} + \sum_{\varsigma=1}^{k_2} a_{\omega\varsigma}(p_\omega(t)) \\
&\times f_\varsigma(q_\varsigma(t)) + \sum_{\varsigma=1}^{k_2} b_{\omega\varsigma}(p_\omega(t)) f_\varsigma(q_\varsigma(t-\tau(t))) \\
&+ \sum_{\varsigma=1}^{k_2} \theta_{\omega\varsigma}(p_\omega(t)) \int_{t-\eta(t)}^{t} f_\varsigma(q_\varsigma(s))\mathrm{d}s \\
&+ \Gamma_\omega + v_\omega(t), \\
\frac{\mathrm{d}^2 q_\varsigma(t)}{\mathrm{d}t^2} =& - \alpha_\varsigma q_\varsigma(t) - \beta_\varsigma \frac{\mathrm{d}q_\varsigma(t)}{\mathrm{d}t} + \sum_{\omega=1}^{k_1} c_{\varsigma\omega}(q_\varsigma(t)) \\
&\times g_\omega(p_\omega(t)) + \sum_{\omega=1}^{k_1} d_{\varsigma\omega}(q_\varsigma(t)) g_\omega(p_\omega(t-\sigma(t))) \\
&+ \sum_{\omega=1}^{k_1} \vartheta_{\varsigma\omega}(q_\varsigma(t)) \int_{t-\iota(t)}^{t} g_\omega(p_\omega(s))\mathrm{d}s \\
&+ \Upsilon_\varsigma + u_\varsigma(t), \omega \in \mathfrak{D}, \varsigma \in \Re, t \geq 0, \qquad (7)
\end{aligned}
$$

where

$$
\begin{aligned}
a_{\omega\varsigma}(p_\omega(t)) &= \begin{cases} a^+_{\omega\varsigma}, \phi_{\omega\varsigma} \frac{\mathrm{d}f_\varsigma(p_\varsigma(t))}{\mathrm{d}t} \leq \frac{\mathrm{d}p_\omega(t)}{\mathrm{d}t} \\ a^-_{\omega\varsigma}, \phi_{\omega\varsigma} \frac{\mathrm{d}f_\varsigma(p_\varsigma(t))}{\mathrm{d}t} > \frac{\mathrm{d}p_\omega(t)}{\mathrm{d}t} \end{cases} \\
b_{\omega\varsigma}(p_\omega(t)) &= \begin{cases} b^+_{\omega\varsigma}, \phi_{\omega\varsigma} \frac{\mathrm{d}f_\varsigma(p_\varsigma(t-\tau(t)))}{\mathrm{d}t} \leq \frac{\mathrm{d}p_\omega(t)}{\mathrm{d}t} \\ b^-_{\omega\varsigma}, \phi_{\omega\varsigma} \frac{\mathrm{d}f_\varsigma(p_\varsigma(t-\tau(t)))}{\mathrm{d}t} > \frac{\mathrm{d}p_\omega(t)}{\mathrm{d}t} \end{cases} \\
\theta_{\omega\varsigma}(p_\omega(t)) &= \begin{cases} \theta^+_{\omega\varsigma}, \phi_{\omega\varsigma} \frac{\mathrm{d}\int_{t-\eta(t)}^{t} f_\varsigma(p_\varsigma(s))ds}{\mathrm{d}t} \leq \frac{\mathrm{d}p_\omega(t)}{\mathrm{d}t} \\ \theta^-_{\omega\varsigma}, \phi_{\omega\varsigma} \frac{\mathrm{d}\int_{t-\eta(t)}^{t} f_\varsigma(p_\varsigma(s))ds}{\mathrm{d}t} > \frac{\mathrm{d}p_\omega(t)}{\mathrm{d}t} \end{cases}
\end{aligned} \qquad (8)
$$

$$
\begin{aligned}
c_{\varsigma\omega}(q_\varsigma(t)) &= \begin{cases} c^+_{\varsigma\omega}, \phi_{\varsigma\omega} \frac{\mathrm{d}g_\omega(q_\omega(t))}{\mathrm{d}t} \leq \frac{\mathrm{d}q_\varsigma(t)}{\mathrm{d}t} \\ c^-_{\varsigma\omega}, \phi_{\varsigma\omega} \frac{\mathrm{d}g_\omega(q_\omega(t))}{\mathrm{d}t} > \frac{\mathrm{d}q_\varsigma(t)}{\mathrm{d}t} \end{cases} \\
d_{\varsigma\omega}(q_\varsigma(t)) &= \begin{cases} d^+_{\varsigma\omega}, \phi_{\varsigma\omega} \frac{\mathrm{d}g_\omega(q_\omega(t-\sigma(t)))}{\mathrm{d}t} \leq \frac{\mathrm{d}q_\varsigma(t)}{\mathrm{d}t} \\ d^-_{\varsigma\omega}, \phi_{\varsigma\omega} \frac{\mathrm{d}g_\omega(q_\omega(t-\sigma(t)))}{\mathrm{d}t} > \frac{\mathrm{d}q_\varsigma(t)}{\mathrm{d}t} \end{cases} \\
\vartheta_{\varsigma\omega}(q_\varsigma(t)) &= \begin{cases} \vartheta^+_{\varsigma\omega}, \phi_{\varsigma\omega} \frac{\mathrm{d}\int_{t-\iota(t)}^{t} g_\omega(q_\omega(s))ds}{\mathrm{d}t} \leq \frac{\mathrm{d}q_\varsigma(t)}{\mathrm{d}t} \\ \vartheta^-_{\varsigma\omega}, \phi_{\varsigma\omega} \frac{\mathrm{d}\int_{t-\iota(t)}^{t} g_\omega(q_\omega(s))ds}{\mathrm{d}t} > \frac{\mathrm{d}q_\varsigma(t)}{\mathrm{d}t} \end{cases}
\end{aligned} \qquad (9)
$$

where $p_\omega(t)$ is the ω-th neural status, $q_\varsigma(t)$ is the ς-th neural status, the other parameters remain consistent with those in BAM-IMNNs (1). And the initial data of BAM-IMNNs (7) are prescribed as $p_\omega(\ddagger) = \chi^*_\omega(\ddagger), \dot{I}_\omega(\ddagger) = \varphi^*_\omega(\ddagger)$,$q_\varsigma(\ddagger) = \tilde{\chi}^*_\varsigma(\ddagger), \dot{J}_\varsigma(\ddagger) = \tilde{\varphi}^*_\varsigma(\ddagger)$ and $\chi^*_\omega(\ddagger), \varphi^*_\omega(\ddagger) \in \mathcal{C}([-\S, 0], \mathbf{R}), \ddagger \in [-\S, 0]$, $\tilde{\chi}^*_\varsigma(\ddagger), \tilde{\varphi}^*_\varsigma(\ddagger) \in \mathcal{C}([-\S^*, 0], \mathbf{R}), \ddagger \in [-\S^*, 0], \omega \in \mathfrak{D}, \varsigma \in \Re$.

$e_{1\omega}(t) = p_\omega(t) + x_\omega(t)$, $e_{2\varsigma}(t) = q_\varsigma(t) + y_\varsigma(t)$ stand for synchronization error state, then we have error model of BAM-IMNNs (1) and (7) below:

$$
\begin{aligned}
\frac{\mathrm{d}^2 e_{1\omega}(t)}{\mathrm{d}t^2} =& - \lambda_\omega e_{1\omega}(t) - \mu_\omega \frac{\mathrm{d}e_{1\omega}(t)}{\mathrm{d}t} + \sum_{\varsigma=1}^{k_2} \tilde{a}_{\omega\varsigma}(t) f_\varsigma(q_\varsigma(t)) \\
&+ \sum_{\varsigma=1}^{k_2} \tilde{b}_{\omega\varsigma}(t) f_\varsigma(q_\varsigma(t-\tau(t))) + \sum_{\varsigma=1}^{k_2} \tilde{\theta}_{\omega\varsigma}(t) \\
&\times \int_{t-\eta(t)}^{t} f_\varsigma(q_\varsigma(s))\mathrm{d}s + \sum_{\varsigma=1}^{k_2} a_{\omega\varsigma}(t) f_\varsigma(y_\varsigma(t))
\end{aligned}
$$

$$+\sum_{\varsigma=1}^{k_2} b_{\omega\varsigma}(t)f_\varsigma(y_\varsigma(t-\tau(t)))+\sum_{\varsigma=1}^{k_2}\theta_{\omega\varsigma}(t)$$
$$\times\int_{t-\eta(t)}^{t} f_\varsigma(y_\varsigma(s))\mathrm{d}s+(1+)\Gamma_\omega+v_\omega(t)$$
$$\frac{\mathrm{d}^2e_{2\varsigma}(t)}{\mathrm{d}t^2}=-\alpha_\varsigma e_{2\varsigma}(t)-\beta_\varsigma\frac{\mathrm{d}e_{2\varsigma}(t)}{\mathrm{d}t}+\sum_{\omega=1}^{k_1}\tilde{c}_{\varsigma\omega}(t)g_\omega(p_\omega(t))$$
$$+\sum_{\omega=1}^{k_1}\tilde{d}_{\varsigma\omega}(t)g_\omega(p_\omega(t-\sigma(t)))+\sum_{\omega=1}^{k_1}\tilde{\vartheta}_{\varsigma\omega}(t)$$
$$\times\int_{t-\iota(t)}^{t} g_\omega(p_\omega(s))\mathrm{d}s+\sum_{\omega=1}^{k_1}c_{\varsigma\omega}(t)g_\omega(x_\omega(t))$$
$$+\sum_{\omega=1}^{k_1}d_{\varsigma\omega}(t)g_\omega(x_\omega(t-\sigma(t)))+\sum_{\omega=1}^{k_1}\vartheta_{\varsigma\omega}(t)$$
$$\times\int_{t-\iota(t)}^{t} g_\omega(x_\omega(s))\mathrm{d}s+(1+)\Upsilon_\varsigma+u_\varsigma(t),$$
$$\omega\in\mathfrak{D},\varsigma\in\Re,t\geq 0, \tag{10}$$

where $\tilde{a}_{\omega\varsigma}(t)\in co[a_{\omega\varsigma}(p_\omega(t))]$, $\tilde{b}_{\omega\varsigma}(t)\in co[b_{\omega\varsigma}(p_\omega(t))]$, $\tilde{\theta}_{\omega\varsigma}(t)\in co[\theta_{\omega\varsigma}(p_\omega(t))]$, $\tilde{c}_{\varsigma\omega}(t)\in co[c_{\varsigma\omega}(q_\varsigma(t))]$, $\tilde{d}_{\varsigma\omega}(t)\in co[d_{\varsigma\omega}(q_\varsigma(t))]$, $\tilde{\vartheta}_{\varsigma\omega}(t)\in co[\vartheta_{\varsigma\omega}(q_\varsigma(t))]$.

2.4 lemmas and Definitions

Definition 2 ([10]). The BAM-IMNNs (1) and (7) are said fixed-time anti-synchronization, if for $\forall e_{1\omega}(t),\dot{e}_{1\omega}(t),e_{2\varsigma}(t),\dot{e}_{2\varsigma}(t)\in\mathbf{R}$, and settling time funtion $T(\tilde{e}_{1\omega}(0),\tilde{e}_{2\varsigma}(0))\geq 0$, exist $T_{max}>0$. Such that $T(\tilde{e}_{1\omega}(0),\tilde{e}_{2\varsigma}(0))\leq T_{max}$, and $lim_{t\to T_{max}}||\tilde{e}_{1\omega}(t)||=0$, $lim_{t\to T_{max}}||\tilde{e}_{2\varsigma}(t)||=0$, and $||\tilde{e}_{1\omega}(t)||=0,||\tilde{e}_{2\varsigma}(t)||=0$ for $t>T_{max}$, where $\tilde{e}_{1\omega}(t)=(e_{11}(t),e_{12}(t),...e_{1k_1}(t),\dot{e}_{11}(t),...\dot{e}_{1k_1}(t))^T$, $\tilde{e}_{1\omega}(0)=(e_{11}(0),e_{12}(0),...e_{1k_1}(0),\dot{e}_{11}(0),...\dot{e}_{1k_1}(0))^T$, $\tilde{e}_{2\varsigma}(t)=(e_{21}(t),e_{22}(t),...e_{2k_2}(t),\dot{e}_{21}(t),...\dot{e}_{2k_2}(t))^T$, $\tilde{e}_{2\varsigma}(0)=(e_{21}(0),e_{22}(0),...e_{2k_2}(0),\dot{e}_{21}(0),...\dot{e}_{2k_2}(0))^T$, and T_{max} is named settling time.

Definition 3. ([38]) Suppose the BAM-IMNNs (1) and (7) are fixed-time anti-synchronization, if error system (10) is fixed-time stable, and for a constant $T_p>0$, and $\forall\tilde{e}_{1\omega}(0),\tilde{e}_{2\varsigma}(0)\in\mathbf{R}^{2k}$, such that $T(\tilde{e}_{1\omega}(0),\tilde{e}_{2\varsigma}(0))\leq T_p$, then BAM-IMNNs (1) and (7) are called PTAS, and T_p is called the preassigned-time.

Lemma 1 ([10]). Let $x_1,x_2,...x_n\geq 0,0<\imath_1<1,\imath_2>1$ and such that.

$$\sum_{r=1}^{n}x_r^{\imath_1}\geq(\sum_{r=1}^{n}x_r)^{\imath_1},\sum_{r=1}^{n}x_r^{\imath_2}\geq n(\sum_{r=1}^{n}x_r/n)^{\imath_2}. \tag{11}$$

Lemma 2 ([37]). All for function $\forall V(\cdot):\mathbf{R}^{2k}\to[0,+\infty)$, regular function with positive-define and radially unbounded, and pretty much all results of (10) fulfill

$$\frac{\mathrm{d}V(\tilde{e}(t))}{\mathrm{d}t}\leq-\gamma V^\epsilon(\tilde{e}(t))-\varpi V^l(\tilde{e}(t))+AV(\tilde{e}(t))-\varXi$$

in which $\gamma,\varpi,\varXi,A>0,A<min\Big\{\gamma,\varpi\Big\},0<\epsilon<1,l>1$, then. system (10) is fixed-time stable and ST is

$$T_{max}=\frac{[(\gamma-A)^{\frac{1}{\epsilon}}+\varXi^{\frac{1}{\epsilon}}]^{1-\epsilon}-\varXi^{\frac{1-\epsilon}{\epsilon}}}{(\gamma-A)^{\frac{1}{\epsilon}}(1-\epsilon)}+\frac{[(\gamma+\varXi)^{\frac{1}{l}}+(\varpi-A)^{\frac{1}{l}}]^{1-l}}{2^{1-l}(l-1)(\varpi-A)^{\frac{1}{l}}},A>0, \tag{12}$$

Lemma 3 ([38]). Let $\forall V(\cdot):\mathbf{R}^{2k}\to[0,+\infty)$, which is the regular function with radially unbounded and positive-define, and pretty much all results of (10) fulfill

$$\frac{\mathrm{d}V(\tilde{e}(t))}{\mathrm{d}t}\leq\frac{T_{max}}{T_p}(-\gamma V^\epsilon(\tilde{e}(t))-\varpi V^l(\tilde{e}(t))+AV(\tilde{e}(t))-\varXi)$$

then. BAM-IMNNs (1) and (7) can implement PTAS, and T_p is called preassigned-time.

Remark 1. It is worth noting that the definitions and lemmas given in this subsection are the main basis for the research results of this paper, and they are also clearly marked in the derivation part of this paper.

3 Main results

3.1 PTAS between drive-response BAM-IMNNs (1) and (7)

We get some results on PTAS between BAM-IMNNs (1) and (7) in this part, we firstly design the following controller to achieve this goal.

$$v_\omega(t)=-m_\omega e_{1\omega}(t)-n_\omega\dot{e}_{1\omega}(t)-\frac{T_{max}}{T_p}sign(\dot{e}_{1\omega}(t))$$
$$\times(\kappa_{1\omega}|e_{1\omega}(t)|^\epsilon+\kappa_{2\omega}|\dot{e}_{1\omega}(t)|^\epsilon+\kappa_{3\omega}|e_{1\omega}(t)|^l$$
$$+\kappa_{4\omega}|\dot{e}_{1\omega}(t)|^l)+\tilde{A}(\frac{T_{max}}{T_p}-1)(sign(\dot{e}_{1\omega}(t))$$
$$\times|e_{1\omega}(t)|+\dot{e}_{1\omega}(t))-sign(\dot{e}_{1\omega}(t))(\tilde{\varXi}\frac{T_{max}}{T_p}$$
$$+\aleph_\omega)-2\Gamma_\omega,$$

$$\begin{aligned}
u_\varsigma(t) =& - m_\varsigma^* e_{2\varsigma}(t) - n_\varsigma^* \dot{e}_{2\varsigma}(t) - \frac{T_{max}}{T_p} sign(\dot{e}_{2\varsigma}(t)) \\
& \times (\pi_{1\varsigma}|e_{2\varsigma}(t)|^\epsilon + \pi_{2\varsigma}|\dot{e}_{2\varsigma}(t)|^\epsilon + \pi_{3\varsigma}|e_{2\varsigma}(t)|^l \\
& + \pi_{4\varsigma}|\dot{e}_{2\varsigma}(t)|^l) + \tilde{A}^*(\frac{T_{max}}{T_p} - 1)(sign(\dot{e}_{2\varsigma}(t)) \\
& \times |e_{2\varsigma}(t)| + \dot{e}_{2\varsigma}(t)) - sign(\dot{e}_{2\varsigma}(t))(\tilde{\Xi}^* \frac{T_{max}}{T_p} \\
& + \aleph_\varsigma) - 2\Upsilon_\varsigma, \qquad (13)
\end{aligned}$$

where $m_\omega, n_\omega, \kappa_{1\omega}, \kappa_{2\omega}, \kappa_{3\omega}, \kappa_{4\omega}, m_\varsigma^*, n_\varsigma^*, \pi_{1\varsigma}, \pi_{2\varsigma}, \pi_{3\varsigma}, \pi_{4\varsigma}$ are all non-negative constants, and T_{max} is settling time of fixed-time anti-synchronization, T_p is preassigned-time, we let

$$\tilde{A} = \max_{1\le\omega\le k_1} \Big\{1 - \mu_\omega - n_\omega, \lambda_\omega + m_\omega\Big\}, \qquad (14)$$

$$\tilde{\gamma} = \min_{1\le\omega\le k_1} \Big\{\kappa_{1\omega}, \kappa_{2\omega}\Big\}, \qquad (15)$$

$$\tilde{\varpi} = (2k_1)^{1-l} \min_{1\le\omega\le k_1} \Big\{\kappa_{3\omega}, \kappa_{4\omega}\Big\}, \qquad (16)$$

$$\tilde{\Xi} = \sum_{\omega=1}^{k_1}[E_\omega - \sum_{\varsigma=1}^{k_2} 2(A_{\omega\varsigma} + B_{\omega\varsigma} + \theta\eta)\Pi_\varsigma], \qquad (17)$$

$$\aleph_\omega = \sum_{\varsigma=1}^{k_2} 2(A_{\omega\varsigma} + B_{\omega\varsigma} + \theta\eta)\Pi_\varsigma, \qquad (18)$$

$$\tilde{A}^* = \max_{1\le\varsigma\le k_2} \Big\{1 - \beta_\varsigma - n_\varsigma^*, \alpha_\varsigma + m_\varsigma^*\Big\}, \qquad (19)$$

$$\tilde{\gamma}^* = \min_{1\le\varsigma\le k_2} \Big\{\pi_{1\varsigma}, \pi_{2\varsigma}\Big\}, \qquad (20)$$

$$\tilde{\varpi}^* = (2k_2)^{1-l} \min_{1\le\varsigma\le k_2} \Big\{\pi_{3\varsigma}, \pi_{4\varsigma}\Big\}, \qquad (21)$$

$$\tilde{\Xi}^* = \sum_{\varsigma=1}^{k_2}[E_\varsigma^* - \sum_{\omega=1}^{k_1} 2(C_{\varsigma\omega} + D_{\varsigma\omega} + \vartheta\iota)\Pi_\omega], \qquad (22)$$

$$\aleph_\varsigma = \sum_{\omega=1}^{k_1} 2(C_{\varsigma\omega} + D_{\varsigma\omega} + \vartheta\iota)\Pi_\omega, \qquad (23)$$

$$\begin{aligned}
& A = \max\Big\{\tilde{A}, \tilde{A}^*\Big\}, \gamma = \min\Big\{\tilde{\gamma}, \tilde{\gamma}^*\Big\}, \\
& \varpi = \min\Big\{\tilde{\varpi}, \tilde{\varpi}^*\Big\}, \Xi = \tilde{\Xi} + \tilde{\Xi}^*, \qquad (24)
\end{aligned}$$

Theorem 1. If **Assumption1** holds true, and $\gamma, \varpi, \Xi, A > 0$, $A < \min\Big\{\gamma, \varpi\Big\}$ hold, then BAM-IMNNs (1) and (7) can implement PTAS, and preassigned-time is T_p.

Proof. We design positive function

$$V(t) = V_1(t) + V_2(t)$$

where

$$V_1(t) = \sum_{\omega=1}^{k_1}(|e_{1\omega}(t)| + |\dot{e}_{1\omega}(t)|)$$

$$V_2(t) = \sum_{\varsigma=1}^{k_2}(|e_{2\varsigma}(t)| + |\dot{e}_{2\varsigma}(t)|)$$

Along solutions of error system (13) and through calculation analysis, we get

$$\begin{aligned}
D^+V(t) =& D^+V_1(t) + D^+V_2(t) \\
=& \sum_{\omega=1}^{k_1}[\dot{e}_{1\omega}(t)sign(e_{1\omega}(t)) + \ddot{e}_{1\omega}(t)sign(\dot{e}_{1\omega}(t))] \\
& + \sum_{\varsigma=1}^{k_2}[\dot{e}_{2\varsigma}(t)sign(e_{2\varsigma}(t)) + \ddot{e}_{2\varsigma}(t)sign(\dot{e}_{2\varsigma}(t))] \\
=& \sum_{\omega=1}^{k_1}\Big\{sign(e_{1\omega}(t))\dot{e}_{1\omega}(t) + sign(\dot{e}_{1\omega}(t))[-\lambda_\omega \\
& e_{1\omega}(t) - \mu_\omega \dot{e}_{1\omega}(t) + \sum_{\varsigma=1}^{k_2} \tilde{a}_{\omega\varsigma}(t) f_\varsigma(q_\varsigma(t)) + \sum_{\varsigma=1}^{k_2} \tilde{b}_{\omega\varsigma}(t) \\
& \times f_\varsigma(q_\varsigma(t-\tau(t))) + \sum_{\varsigma=1}^{k_2} \tilde{\theta}_{\omega\varsigma}(t) \int_{t-\eta(t)}^{t} f_\varsigma(q_\varsigma(s))\mathrm{d}s \\
& + \sum_{\varsigma=1}^{k_2} a_{\omega\varsigma}(t) f_\varsigma(y_\varsigma(t)) + \sum_{\varsigma=1}^{k_2} b_{\omega\varsigma}(t) f_\varsigma(y_\varsigma(t-\tau(t))) \\
& + \sum_{\varsigma=1}^{k_2} \theta_{\omega\varsigma}(t) \int_{t-\eta(t)}^{t} f_\varsigma(y_\varsigma(s))\mathrm{d}s + 2\Gamma_\omega - m_\omega e_{1\omega}(t) \\
& - n_\omega \dot{e}_{1\omega}(t) - \frac{T_{max}}{T_p} sign(\dot{e}_{1\omega}(t))(\kappa_{1\omega}|e_{1\omega}(t)|^\epsilon \\
& + \kappa_{2\omega}|\dot{e}_{1\omega}(t)|^\epsilon + \kappa_{3\omega}|e_{1\omega}(t)|^l + \kappa_{4\omega}|\dot{e}_{1\omega}(t)|^l) \\
& + \tilde{A}(\frac{T_{max}}{T_p} - 1)(sign(\dot{e}_{1\omega}(t))|e_{1\omega}(t)| + \dot{e}_{1\omega}(t)) \\
& - sign(\dot{e}_{1\omega}(t))(\tilde{\Xi}\frac{T_{max}}{T_p} + \aleph_\omega) - 2\Gamma_\omega]\Big\} \\
& + \sum_{\varsigma=1}^{k_2}\Big\{sign(e_{2\varsigma}(t))\dot{e}_{2\varsigma}(t) + sign(\dot{e}_{2\varsigma}(t))[-\alpha_\varsigma e_{2\varsigma}(t) \\
& - \beta_\varsigma \dot{e}_{2\varsigma}(t) + \sum_{\omega=1}^{k_1} \tilde{c}_{\varsigma\omega}(t) g_\omega(p_\omega(t)) + \sum_{\omega=1}^{k_1} \tilde{d}_{\varsigma\omega}(t) \\
& \times g_\omega(p_\omega(t-\sigma(t))) + \sum_{\omega=1}^{k_1} \tilde{\vartheta}_{\varsigma\omega}(t) \int_{t-\iota(t)}^{t} g_\omega(p_\omega(s))\mathrm{d}s
\end{aligned}$$

$$
\begin{aligned}
&+\sum_{\omega=1}^{k_1} c_{\varsigma\omega}(t)g_\omega(x_\omega(t))+\sum_{\omega=1}^{k_1} d_{\varsigma\omega}(t)g_\omega(x_\omega(t-\sigma(t)))\\
&+\sum_{\omega=1}^{k_1}\vartheta_{\varsigma\omega}(t)\int_{t-\iota(t)}^{t} g_\omega(x_\omega(s))\mathrm{d}s+2\Upsilon_\varsigma-m_\varsigma^* e_{2\varsigma}(t)\\
&-n_\varsigma^*\dot e_{2\varsigma}(t)-\frac{T_{max}}{T_p}sign(\dot e_{2\varsigma}(t))(\pi_{1\varsigma}|e_{2\varsigma}(t)|^\epsilon\\
&+\pi_{2\varsigma}|\dot e_{2\varsigma}(t)|^\epsilon+\pi_{3\varsigma}|e_{2\varsigma}(t)|^l+\pi_{4\varsigma}|\dot e_{2\varsigma}(t)|^l)\\
&+\tilde A^*(\frac{T_{max}}{T_p}-1)(sign(\dot e_{2\varsigma}(t))|e_{2\varsigma}(t)|+\dot e_{2\varsigma}(t))\\
&-sign(\dot e_{2\varsigma}(t))(\tilde\Xi^*\frac{T_{max}}{T_p}+\aleph_\varsigma)-2\Upsilon_\varsigma]\Big\}. \qquad (25)
\end{aligned}
$$

From **Asummption1** and (25), by directly scaling or shrinking the activation function, connection weight and sign function, we get

$$
\begin{aligned}
D^+V(t)\leqslant&\sum_{\omega=1}^{k_1}\Big\{|\dot e_{1\omega}(t)|+\lambda_\omega|e_{1\omega}(t)|-\mu_\omega|\dot e_{1\omega}(t)|\\
&+2\sum_{\varsigma=1}^{k_2}(A_{\omega\varsigma}+B_{\omega\varsigma}+\theta\eta)\Pi_\varsigma+m_\omega|e_{1\omega}(t)|\\
&-n_\omega|\dot e_{1\omega}(t)|-\frac{T_{max}}{T_p}(\kappa_{1\omega}|e_{1\omega}(t)|^\epsilon+\kappa_{2\omega}|\dot e_{1\omega}(t)|^\epsilon\\
&+\kappa_{3\omega}|e_{1\omega}(t)|^l+\kappa_{4\omega}|\dot e_{1\omega}(t)|^l)+\tilde A(\frac{T_{max}}{T_p}-1)\\
&(|e_{1\omega}(t)|+|\dot e_{1\omega}(t)|)-(\tilde\Xi\frac{T_{max}}{T_p}+\aleph_\omega)\Big\}\\
&+\sum_{\varsigma=1}^{k_2}\Big\{|\dot e_{2\varsigma}(t)|+\alpha_\varsigma|e_{2\varsigma}(t)|-\beta_\varsigma|\dot e_{2\varsigma}(t)|\\
&+2\sum_{\omega=1}^{k_1}(C_{\varsigma\omega}+D_{\varsigma\omega}+\vartheta\iota)\Pi_\omega+m_\varsigma^*|e_{2\varsigma}(t)|\\
&-n_\varsigma^*|\dot e_{2\varsigma}(t)|-\frac{T_{max}}{T_p}(\pi_{1\varsigma}|e_\varsigma(t)|^\epsilon+\pi_{2\varsigma}|\dot e_{2\varsigma}(t)|^\epsilon\\
&+\pi_{3\varsigma}|e_{2\varsigma}(t)|^l+\pi_{4\varsigma}|\dot e_{2\varsigma}(t)|^l)+\tilde A^*(\frac{T_{max}}{T_p}-1)\\
&(|e_{2\varsigma}(t)|+|\dot e_{2\varsigma}(t)|)-(\tilde\Xi^*\frac{T_{max}}{T_p}+\aleph_\varsigma)\Big\}\\
=&\sum_{\omega=1}^{k_1}\Big\{(1-\mu_\omega-n_\omega)|\dot e_{1\omega}(t)|+(\lambda_\omega+m_\omega)\\
&|e_{1\omega}(t)|+2\sum_{\varsigma=1}^{k_2}(A_{\omega\varsigma}+B_{\omega\varsigma}+\theta\eta)\Pi_\varsigma-\frac{T_{max}}{T_p}\\
&(\kappa_{1\omega}|e_{1\omega}(t)|^\epsilon+\kappa_{2\omega}|\dot e_{1\omega}(t)|^\epsilon+\kappa_{3\omega}|e_{1\omega}(t)|^l\\
&+\kappa_{4\omega}|\dot e_{1\omega}(t)|^l)+\tilde A(\frac{T_{max}}{T_p}-1)(|e_{1\omega}(t)|\\
&+|\dot e_{1\omega}(t)|)-(\tilde\Xi\frac{T_{max}}{T_p}+\aleph_\omega)\Big\}\\
&+\sum_{\varsigma=1}^{k_2}\Big\{(1-\beta_\varsigma-n_\varsigma^*)|\dot e_{2\varsigma}(t)|+(\alpha_\varsigma+m_\varsigma^*)\\
&|e_{2\varsigma}(t)|+2\sum_{\omega=1}^{k_1}(C_{\varsigma\omega}+D_{\varsigma\omega}+\vartheta\iota)\Pi_\omega-\frac{T_{max}}{T_p}\\
&(\pi_{1\varsigma}|e_\varsigma(t)|^\epsilon+\pi_{2\varsigma}|\dot e_{2\varsigma}(t)|^\epsilon+\pi_{3\varsigma}|e_{2\varsigma}(t)|^l\\
&+\pi_{4\varsigma}|\dot e_{2\varsigma}(t)|^l)+\tilde A^*(\frac{T_{max}}{T_p}-1)(|e_{2\varsigma}(t)|\\
&+|\dot e_{2\varsigma}(t)|)-(\tilde\Xi^*\frac{T_{max}}{T_p}+\aleph_\varsigma)\Big\}\\
&. \qquad (26)
\end{aligned}
$$

Basing on **Lemma 1**, (15), (16), (20) and (21), we get

$$
\begin{aligned}
&-\sum_{\omega=1}^{k_1}(\kappa_{1\omega}|e_{1\omega}(t)|^\epsilon+\kappa_{2\omega}|\dot e_{1\omega}(t)|^\epsilon)\\
&\le-\gamma[\sum_{\omega=1}^{k_1}(|e_{1\omega}(t)|+|\dot e_{1\omega}(t)|)]^\epsilon\\
&-\sum_{\omega=1}^{k_1}(\kappa_{3\omega}|e_{1\omega}(t)|^l+\kappa_{4\omega}|\dot e_{1\omega}(t)|^l)\\
&\le-\varpi[\sum_{\omega=1}^{k_1}(|e_{1\omega}(t)|+|\dot e_{1\omega}(t)|)]^l.\\
&-\sum_{\varsigma=1}^{k_2}(\pi_{1\varsigma}|e_{2\varsigma}(t)|^\epsilon+\pi_{2\varsigma}|\dot e_{2\varsigma}(t)|^\epsilon)\\
&\le-\gamma^*[\sum_{\varsigma=1}^{k_2}(|e_{2\varsigma}(t)|+|\dot e_{2\varsigma}(t)|)]^\epsilon\\
&-\sum_{\varsigma=1}^{k_2}(\pi_{3\varsigma}|e_{2\varsigma}(t)|^l+\pi_{4\varsigma}|\dot e_{2\varsigma}(t)|^l)\\
&\le-\varpi^*[\sum_{\varsigma=1}^{k_2}(|e_{2\varsigma}(t)|+|\dot e_{2\varsigma}(t)|)]. \qquad (27)
\end{aligned}
$$

we get

$$
\begin{aligned}
D^+V(t)=&\sum_{\omega=1}^{k_1}\Big\{(1-\mu_\omega-n_\omega)|\dot e_{1\omega}(t)|+(\lambda_\omega+m_\omega)\\
&|e_{1\omega}(t)|+2\sum_{\varsigma=1}^{k_2}(A_{\omega\varsigma}+B_{\omega\varsigma}+\theta\eta)\Pi_\varsigma+\frac{T_{max}}{T_p}\\
&(-\gamma[\sum_{\omega=1}^{k_1}(|e_{1\omega}(t)|+|\dot e_{1\omega}(t)|)]^\epsilon-\varpi[\sum_{\omega=1}^{k_1}(|e_{1\omega}(t)|
\end{aligned}
$$

$$+|\dot{e}_{1\omega}(t)|)]^{l})+\tilde{A}(\frac{T_{max}}{T_p}-1)(|e_{1\omega}(t)|$$
$$+|\dot{e}_{1\omega}(t)|)-(\tilde{\Xi}\frac{T_{max}}{T_p}+\aleph_{\omega})\Big\}$$
$$+\sum_{\varsigma=1}^{k_2}\Big\{(1-\beta_{\varsigma}-n_{\varsigma}^{*})|\dot{e}_{2\varsigma}(t)|+(\alpha_{\varsigma}+m_{\varsigma}^{*})$$
$$|e_{2\varsigma}(t)|+2\sum_{\omega=1}^{k_1}(C_{\varsigma\omega}+D_{\varsigma\omega}+\vartheta_{\iota})\Pi_{\omega}+\frac{T_{max}}{T_p}$$
$$(-\gamma^{*}[\sum_{\varsigma=1}^{k_2}(|e_{2\varsigma}(t)|+|\dot{e}_{2\varsigma}(t)|)]^{\epsilon}-\varpi^{*}[\sum_{\varsigma=1}^{k_2}(|e_{2\varsigma}(t)|$$
$$+|\dot{e}_{2\varsigma}(t)|)]^{l})+\tilde{A}^{*}(\frac{T_{max}}{T_p}-1)(|e_{2\varsigma}(t)|$$
$$+|\dot{e}_{2\varsigma}(t)|)-(\tilde{\Xi}^{*}\frac{T_{max}}{T_p}+\aleph_{\varsigma})\Big\}$$

Basing (14), (18), (19) and (23), then

$$D^{+}V_1(t)\leqslant\frac{T_{max}}{T_p}(\tilde{A}V_1(t)-\tilde{\gamma}V_1^{\epsilon}(t)-\tilde{\varpi}V_1^{l}(t)-\tilde{\Xi})$$
$$D^{+}V_2(t)\leqslant\frac{T_{max}}{T_p}(\tilde{A}^{*}V_2(t)-\tilde{\gamma}^{*}V_2^{\epsilon}(t)-\tilde{\varpi}^{*}V_2^{l}(t)-\tilde{\Xi}^{*}).\tag{28}$$

then, one gets

$$D^{+}V(t)\leqslant\frac{T_{max}}{T_p}(AV(t)-\gamma V^{\epsilon}(t)-\varpi V^{l}(t)-\Xi).\tag{29}$$

then, from **Lemma 3**, we get BAM-IMNNs (1) and (7) can attain PTAS under the controller (13). This proof is complete.

Remark 2.

It is worth noting that when $T_p = T_{max}$ in the controller of Theorem1, the preassigned-time anti-synchronization problem we studied can be transformed into a fixed time anti-synchronization problem.

Remark 3.

The Lyapunov function designed in Theorem 1 explicitly includes errors and their derivatives, ensuring that they converge simultaneously and making it particularly suitable for analyzing second-order dynamic systems. And it is a key tool for proving that the system achieves fixed time consistency. Its derivatives can conveniently handle non-smooth terms such as signed functions in the control law. In the research of this article, this type of Lyapunov function is highly in line with our requirements.

Remark 4. The research on preset time anti-synchronization control has solved another type of key problem that traditional synchronization control cannot handle. Its core value lies in enabling the system to achieve anti-synchronization within the precise time set by the user and independent of the initial state of the system. This is crucial for enhancing the security, reliability and performance of the system.

4 Numerical simulations

let's give some simulations results to explain the PTAS as follows.

Example 1. Discuss the two-dimensional BAM-IMNNs is showed below

$$\begin{aligned}
\frac{d^2x_1(t)}{dt^2}=&-1.25x_1(t)-0.1\frac{dx_1(t)}{dt}+\sum_{\varsigma=1}^{2}a_{1\varsigma}(x_1(t))\\
&f_{\varsigma}(y_{\varsigma}(t))+\sum_{\varsigma=1}^{2}b_{1\varsigma}(x_1(t))f_{\varsigma}(y_{\varsigma}(t-\tau(t)))\\
&+\sum_{\varsigma=1}^{2}\theta_{1\varsigma}(x_1(t))\int_{t-\eta(t)}^{t}f_{\varsigma}(y_{\varsigma}(s))ds\\
\frac{d^2x_2(t)}{dt^2}=&-1.25x_2(t)-0.1\frac{dx_2(t)}{dt}+\sum_{\varsigma=1}^{2}a_{2\varsigma}(x_2(t))\\
&f_{\varsigma}(y_{\varsigma}(t))+\sum_{\varsigma=1}^{2}b_{2\varsigma}(x_2(t))f_{\varsigma}(y_{\varsigma}(t-\tau(t)))\\
&+\sum_{\varsigma=1}^{2}\theta_{2\varsigma}(x_2(t))\int_{t-\eta(t)}^{t}f_{\varsigma}(y_{\varsigma}(s))ds\\
\frac{d^2y_1(t)}{dt^2}=&-1.5y_1(t)-0.2\frac{dy_1(t)}{dt}+\sum_{\omega=1}^{2}c_{1\omega}(y_1(t))\\
&g_{\omega}(x_{\omega}(t))+\sum_{\omega=1}^{2}d_{1\omega}(y_1(t))g_{\omega}(x_{\omega}(t-\sigma(t)))\\
&+\sum_{\omega=1}^{2}\vartheta_{1\omega}(y_1(t))\int_{t-\iota(t)}^{t}g_{\omega}(x_{\omega}(s))ds\\
\frac{d^2y_2(t)}{dt^2}=&-1.5y_2(t)-0.2\frac{dy_2(t)}{dt}+\sum_{\omega=1}^{2}c_{2\omega}(y_2(t))\\
&g_{\omega}(x_{\omega}(t))+\sum_{\omega=1}^{2}d_{2\omega}(y_2(t))g_{\omega}(x_{\omega}(t-\sigma(t)))
\end{aligned}$$

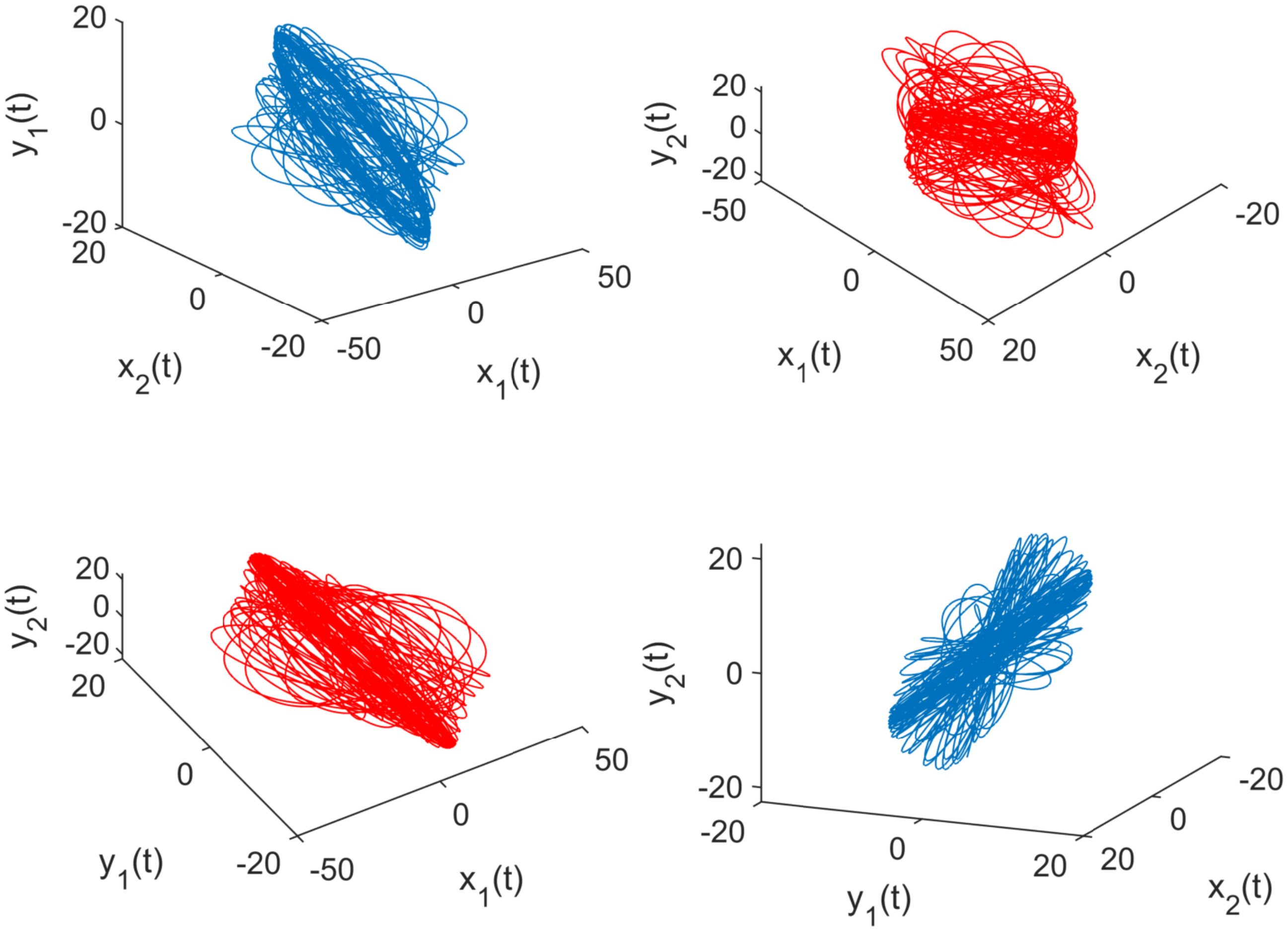

Figure 1. Phase trajectories of BAM-IMNNs (30).

$$+\sum_{\omega=1}^{2}\vartheta_{2\omega}(y_2(t))\int_{t-\iota(t)}^{t} g_\omega(x_\omega(s))\mathrm{d}s, \qquad (30)$$

where $a_{11}(x_1(t)) = 2.2, a_{12}^{+} = 1.6, a_{12}^{-} = 1.8, b_{11}^{+} = -3.24, b_{11}^{-} = -3.2, b_{12}^{+} = 2.82, b_{12}^{-} = 2.83, \theta_{11}^{+} = -0.01, \theta_{11}^{-} = -0.01, \theta_{12}^{+} = 0.01, \theta_{12}^{-} = 0.02, a_{22}(x_2(t)) = -1.6, a_{21}^{+} = -2.4, a_{21}^{-} = -2.6, b_{21}^{+} = -2.5, b_{21}^{-} = -2.45, b_{22}^{+} = 2.8, b_{22}^{-} = 2.87, \theta_{21}^{+} = -0.01, \theta_{21}^{-} = -0.01, \theta_{22}^{+} = 0.01, \theta_{22}^{-} = 0.02, c_{11}(y_1(t)) = 0.6, c_{12}^{+} = -0.5, c_{12}^{-} = -0.3, d_{11}^{+} = 1.6, d_{11}^{-} = 1.62, d_{12}^{+} = -2.5, d_{12}^{-} = -2.9, \vartheta_{11}^{+} = 0.01, \vartheta_{11}^{-} = 0.02, \vartheta_{12}^{+} = -0.05, \vartheta_{12}^{-} = -0.02, c_{22}(y_2(t)) = -1.8, c_{21}^{+} = -1.1, c_{21}^{-} = -1.13, d_{21}^{+} = 1.39, d_{21}^{-} = 1.38, d_{22}^{+} = -3.25, d_{22}^{-} = -3.27, \vartheta_{21}^{+} = 0.01, \vartheta_{21}^{-} = 0.02, \vartheta_{22}^{+} = -0.01, \vartheta_{22}^{-} = -0.02, \tau(t) = \eta(t) = \sigma(t) = \iota(t) = \frac{exp(t)}{1+exp(t)}, g_\omega(x_\omega(t)) = tanh(x_\omega(t)), f_\varsigma(y_\varsigma(t)) = tanh(y_\varsigma(t)), \omega, \varsigma = 1, 2$, and $\Gamma_\omega = \Upsilon_\varsigma = 0$.

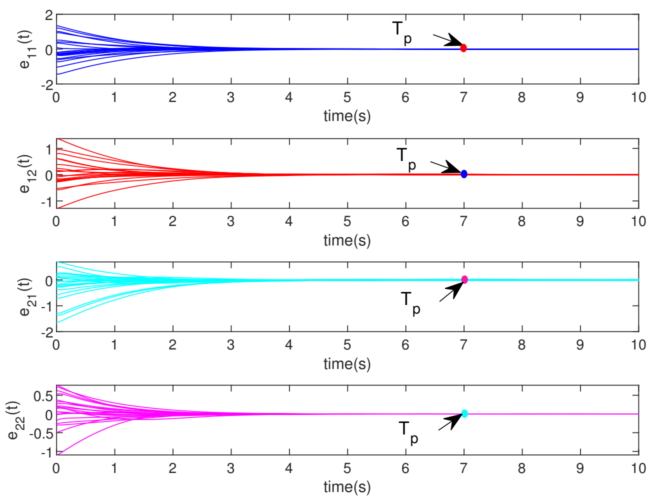

Figure 2. Error trajectories of BAM-IMNNs (30) and (31) with$T_p = 5$.

BAM-IMNNS (30) exists chaotic via initials $\chi_1(\ddagger) = 0.8, \varphi_1(\ddagger) = 0.75, \chi_2(\ddagger) = -0.8, \varphi_2(\ddagger) = -0.65, \tilde{\chi}_1(\ddagger) = 0.5, \tilde{\varphi}_1(\ddagger) = 0.65, \tilde{\chi}_2(\ddagger) = -0.7, \tilde{\varphi}_2(\ddagger) = -0.6, \forall \ddagger \in [-1, 0)$, let's drawn it in Figure 1.

let's give corresponding response systems below

$$
\begin{aligned}
\frac{\mathrm{d}^2 p_1(t)}{\mathrm{d}t^2} =& -1.25 p_1(t) - 0.1 \frac{\mathrm{d}p_1(t)}{\mathrm{d}t} + \sum_{\varsigma=1}^{2} a_{1\varsigma}(p_1(t)) \\
& f_\varsigma(q_\varsigma(t)) + \sum_{\varsigma=1}^{2} b_{1\varsigma}(p_1(t)) f_\varsigma(q_\varsigma(t-\tau(t))) \\
& + \sum_{\varsigma=1}^{2} \theta_{1\varsigma}(p_1(t)) \int_{t-\eta(t)}^{t} f_\varsigma(q_\varsigma(s))\mathrm{d}s + v_1(t), \\
\frac{\mathrm{d}^2 p_2(t)}{\mathrm{d}t^2} =& -1.25 p_2(t) - 0.1 \frac{\mathrm{d}p_2(t)}{\mathrm{d}t} + \sum_{\varsigma=1}^{2} a_{2\varsigma}(p_2(t)) \\
& f_\varsigma(q_\varsigma(t)) + \sum_{\varsigma=1}^{2} b_{2\varsigma}(p_2(t)) f_\varsigma(q_\varsigma(t-\tau(t))) \\
& + \sum_{\varsigma=1}^{2} \theta_{2\varsigma}(p_2(t)) \int_{t-\eta(t)}^{t} f_\varsigma(q_\varsigma(s))\mathrm{d}s + v_2(t), \\
\frac{\mathrm{d}^2 q_1(t)}{\mathrm{d}t^2} =& -1.5 q_1(t) - 0.2 \frac{\mathrm{d}q_1(t)}{\mathrm{d}t} + \sum_{\omega=1}^{2} c_{1\omega}(q_1(t)) \\
& g_\omega(p_\omega(t)) + \sum_{\omega=1}^{2} d_{1\omega}(q_1(t)) g_\omega(p_\omega(t-\sigma(t))) \\
& + \sum_{\omega=1}^{2} \vartheta_{1\omega}(q_1(t)) \int_{t-\iota(t)}^{t} g_\omega(p_\omega(s))\mathrm{d}s + u_1(t), \\
\frac{\mathrm{d}^2 q_2(t)}{\mathrm{d}t^2} =& -1.5 q_2(t) - 0.2 \frac{\mathrm{d}q_2(t)}{\mathrm{d}t} + \sum_{\omega=1}^{2} c_{2\omega}(q_2(t)) \\
& g_\omega(p_\omega(t)) + \sum_{\omega=1}^{2} d_{2\omega}(q_2(t)) g_\omega(p_\omega(t-\sigma(t))) \\
& + \sum_{\omega=1}^{2} \vartheta_{2\omega}(q_2(t)) \int_{t-\iota(t)}^{t} g_\omega(p_\omega(s))\mathrm{d}s + u_2(t),
\end{aligned} \tag{31}
$$

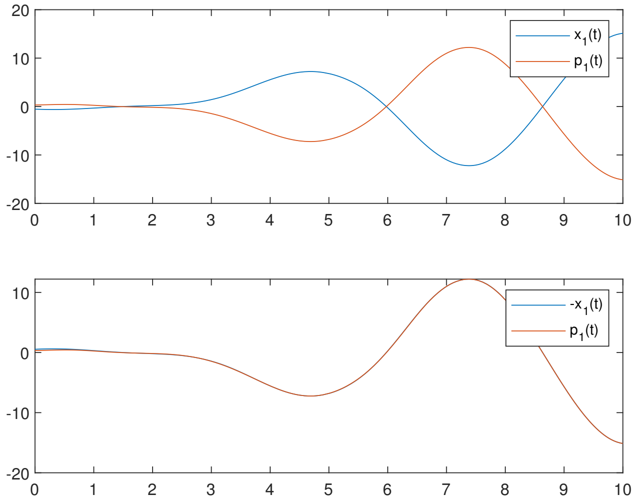

Figure 3. Preassigned-time anti-synchronization trajectories of $x_1(t)$ and $p_1(t)$.

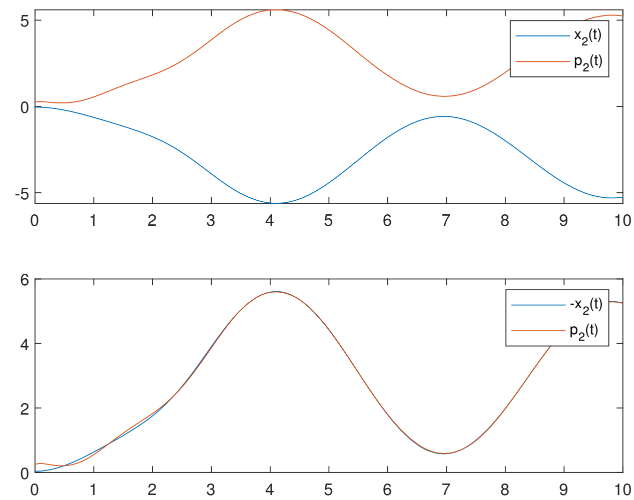

Figure 4. Preassigned-time anti-synchronization trajectories of $x_2(t)$ and $p_2(t)$.

the data of BAM-IMNNs (31) are same as BAM-IMNNs (30), in controller, we let $\tau = \eta = \sigma = \iota = 1, l = 0.5, \epsilon = 1.5, m_1 = m_2 = 14.25, n_1 = n_2 = 1.2, m_1^* = m_2^* = 18.4, n_1^* = n_2^* = 3.3, \kappa_{11} = \kappa_{21} = \kappa_{12} = \kappa_{22} = \pi_{11} = \pi_{21} = \pi_{12} = \pi_{22} = 20, \kappa_{31} = \kappa_{41} = \kappa_{32} = \kappa_{42} = \pi_{31} = \pi_{41} = \pi_{32} = \pi_{42} = 41.6, E_1 = 20.26, E_2 = 19.28, E_1^* = 11.42, E_2^* = 15.3, \tilde{A} = 15.5, \tilde{A}^* = 19.9$. Through simple calculations, we get $A = 19.9, \gamma = 20, \varpi = 20.8, \varXi = 0.24$, And the all requirements of **Theorem 1** hold. Then, system (1) and (7) can get PTAS, and $T_{max} = 5.3937$. Let $T_p = 5 < T_{max} = 5.3937$. Figure 2 shows the error trajectories of BAM-IMNNs (30) and (31) under control, and the traces of state of BAM-IMNNs (30) and (31) are drawed in Figures 3, 4, 5, and 6. Let $T_p = 4 < T_{max} = 5.3937$. Figure 7 shows the error trajectories of BAM-IMNNs (30) and (31) under control.

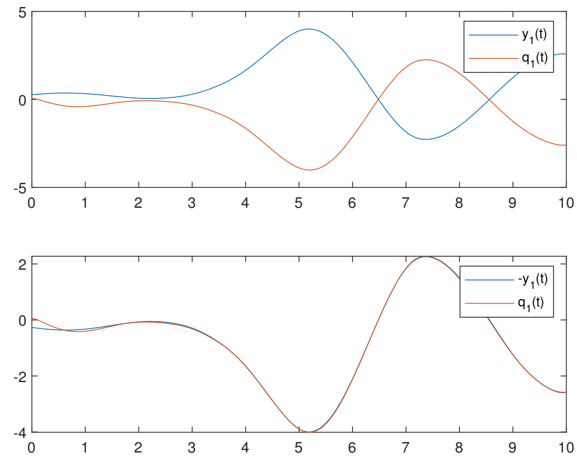

Figure 5. Preassigned-time anti-synchronization trajectories of $y_1(t)$ and $q_1(t)$.

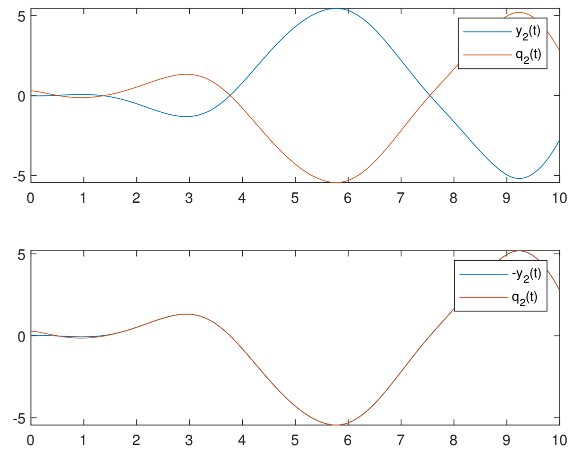

Figure 6. Preassigned-time anti-synchronization trajectories of $y_2(t)$ and $q_2(t)$.

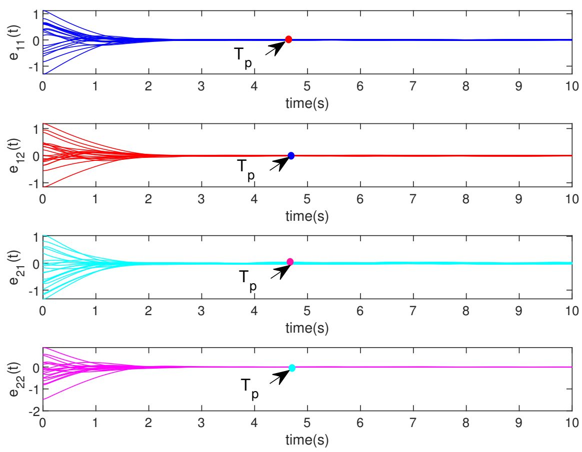

Figure 7. Error trajectories of BAM-IMNNs (30) and (31) with$T_p = 4$.

5 Conclusion

This paper focuses on the preassigned time anti-synchronization control problem of inertial memristor BAM neural networks. By establishing a theoretical framework directly based on second-order differential equations, we have successfully overcome the conservation problem caused by traditional order reduction methods and achieved the complete retention of the dynamic characteristics of the system. Although this research has achieved certain results, there are still issues worthy of further exploration. How to apply theoretical achievements to large-scale neural network systems and develop corresponding hardware acceleration algorithms is a key step towards practical application. These research directions will open up new possibilities for the engineering application of inertial memristor neural networks.

Data Availability Statement

Data will be made available on request.

Funding

This work was supported by the National Science Foundation of China under Grant 62476292, and the Fundamental Research Funds for Central University of South-Central Minzu University under Grant CZQ24020.

Conflicts of Interest

The authors declare no conflicts of interest.

Ethical Approval and Consent to Participate

Not applicable.

References

[1] Song, Q., & Cao, J. (2007). Dynamics of bidirectional associative memory networks with distributed delays and reaction–diffusion terms. *Nonlinear Analysis: Real World Applications*, *8*(1), 345-361. [CrossRef]

[2] Cao, J., & Xiao, M. (2007). Stability and Hopf bifurcation in a simplified BAM neural network with two time delays. *IEEE Transactions on Neural Networks*, *18*(2), 416–430. [CrossRef]

[3] Du, S., Chen, Z., Yuan, Z., & Zhang, X. (2005). Sensitivity to noise in bidirectional associative memory (BAM). *IEEE Transactions on Neural Networks*, *16*(4), 887-898. [CrossRef]

[4] Kosko, B. (2002). Bidirectional associative memories. *IEEE Transactions on Systems, Man, and Cybernetics*, *18*(1), 49–60. [CrossRef]

[5] Kosko, B. (1987). Adaptive bidirectional associative memories. *Applied Optics*, *26*(23), 4947–4960. [CrossRef]

[6] Zhang, Z., & Cao, J. (2021). Finite-time synchronization for fuzzy inertial neural networks by maximum value approach. *IEEE Transactions on Fuzzy Systems*, *30*(5), 1436-1446. [CrossRef]

[7] Zhang, Y., Jiang, M., & Fang, X. (2020). A new fixed-time stability criterion and its application to synchronization control of memristor-based fuzzy inertial neural networks with proportional delay. *Neural Processing Letters*, *52*(2), 1291-1315. [CrossRef]

[8] Ge, J., & Xu, J. (2010). Computation of synchronized periodic solution in a BAM network with two delays. *IEEE Transactions on Neural Networks*, *21*(3), 439–450. [CrossRef]

[9] Duan, L., & Li, J. (2025). Finite-time synchronization for a fully complex-valued BAM inertial neural network with proportional delays via non-reduced order and non-separation approach. *Neurocomputing*, *611*, 128648. [CrossRef]

[10] Duan, L., & Li, J. (2021). Fixed-time synchronization of fuzzy neutral-type BAM memristive inertial neural networks with proportional delays. *Information Sciences*, *576*, 522-541. [CrossRef]

[11] Arslan, E., Narayanan, G., Ali, M. S., Arik, S., & Saroha, S. (2020). Controller design for finite-time and fixed-time stabilization of fractional-order memristive complex-valued BAM neural networks with uncertain parameters and time-varying delays. *Neural Networks*, *130*, 60-74. [CrossRef]

[12] Li, Q., Wei, H., Hua, D., Wang, J., & Yang, J. (2024). Stabilization of semi-Markovian jumping uncertain complex-valued networks with time-varying delay: A sliding-mode control approach. *Neural Processing Letters*, *56*(2), 111. [CrossRef]

[13] Wei, H., Li, Q., Zhu, S., Fan, D., & Zheng, Y. (2025). Event-triggered resilient asynchronous estimation of stochastic Markovian jumping CVNs with missing measurements: A co-design control strategy. *Information Sciences*, *712*, 122167. [CrossRef]

[14] Aram, Z., Jafari, S., Ma, J., Sprott, J. C., Zendehrouh, S., & Pham, V. T. (2017). Using chaotic artificial neural networks to model memory in the brain. *Communications in Nonlinear Science and Numerical Simulation*, *44*, 449-459. [CrossRef]

[15] Tanaka, T., Nakajima, K., & Aoyagi, T. (2020). Effect of recurrent infomax on the information processing capability of input-driven recurrent neural networks. *Neuroscience Research*, *156*, 225–233. [CrossRef]

[16] Deng, W., & Ma, M. (2024). Analysis of the dynamical behavior of discrete memristor-coupled scale-free neural networks. *Chinese Journal of Physics*, *91*, 966–976. [CrossRef]

[17] Babcock, K. L., & Westervelt, R. M. (1987). Dynamics of simple electronic neural networks. *Physica D: Nonlinear Phenomena*, *28*(3), 305-316. [CrossRef]

[18] Xu, C. J., & Zhang, Q. M. (2015). Existence and global exponential stability of anti-periodic solutions for BAM neural networks with inertial term and delay. *Neurocomputing*, *153*, 108–116. [CrossRef]

[19] Tu, Z. W., Cao, J. D., & Hayat, T. (2016). Global exponential stability in Lagrange sense for inertial neural networks with time-varying delays. *Neurocomputing*, *171*, 524–531. [CrossRef]

[20] Zhang, Z. Q., Chen, M., & Li, A. L. (2020). Further study on finite-time synchronization for delayed inertial neural networks via inequality skills. *Neurocomputing*, *373*, 15–23. [CrossRef]

[21] Xiang, J., Ren, J., & Tan, M. (2022). Asymptotical synchronization for complex-valued stochastic switched neural networks under the sampled-data controller via a switching law. *Neurocomputing*, *514*, 414–425. [CrossRef]

[22] Li, L., Liu, X., Tang, M., Zhang, S., & Zhang, X. M. (2021). Asymptotical synchronization analysis of fractional-order complex neural networks with non-delayed and delayed couplings. *Neurocomputing*, *445*, 180-193. [CrossRef]

[23] Chen, D., & Zhang, Z. (2022). Globally asymptotic synchronization for complex-valued BAM neural networks by the differential inequality way. *Chaos, Solitons & Fractals*, *164*, 112681. [CrossRef]

[24] Han, J., & Zhou, L. (2024). Finite-time synchronization of proportional delay memristive competitive neural networks. *Neurocomputing*, *610*, 128612. [CrossRef]

[25] Du, F., Lu, J. G., & Zhang, Q. H. (2024). Practical finite-time synchronization of delayed fuzzy cellular neural networks with fractional-order. *Information Sciences*, *667*, 120457. [CrossRef]

[26] Abdelaziz, M., & Chérif, F. (2024). Finite-time synchronization and exponential lag synchronization of quaternion-valued inertial fuzzy Cohen–Grossberg neural networks with impulsives and mixed delays. *Chaos, Solitons & Fractals*, *180*, 114520. [CrossRef]

[27] Liu, L., Bao, H., & Cao, J. (2024). Adaptive finite-time synchronization of quaternion-valued inertial neural networks with mixed delays under quantized event-triggered impulsive strategy. *Journal of the Franklin Institute*, *361*(12), 107020. [CrossRef]

[28] Zhang, G., Rakkiyappan, R., & Wang, L. (2024). Event-triggered-based fixed/preassigned-time synchronization control of second-order neural networks with distributed delays. *Communications in Nonlinear Science and Numerical Simulation*, *139*, 108301. [CrossRef]

[29] Liu, H., Cheng, J., Cao, J., & Katib, I. (2024). Preassigned-time synchronization for complex-valued memristive neural networks with reaction–diffusion terms and Markov parameters. *Neural Networks*, *169*, 520-531. [CrossRef]

[30] Pu, H., Li, F., Wang, Q., & Li, P. (2023). Preassigned-time projective synchronization of delayed fully quaternion-valued discontinuous neural networks with parameter uncertainties. *Neural Networks*, *165*, 740-754. [CrossRef]

[31] Gao, Y., Yu, J., Hu, C., Wen, S., & Kong, F. (2024). Fixed/preassigned-time output synchronization for T–S fuzzy complex networks via quantized control. *Nonlinear Analysis: Hybrid Systems*, *51*, 101434. [CrossRef]

[32] Zhang, T., Yang, Y., & Han, S. (2025). Exponential heterogeneous anti-synchronization of multi-variable discrete stochastic inertial neural networks with adaptive corrective parameter. *Engineering Applications of Artificial Intelligence*, *142*, 109871. [CrossRef]

[33] Feng, H., Wu, Z., Zhang, X., Xiao, Z., Zhang, M., & Tao, J. (2024). Secure adaptive event-triggered anti-synchronization for BAM neural networks with energy-limited DoS attacks. *Information Sciences*, *670*, 120594. [CrossRef]

[34] Li, X., Liu, X., & Wang, F. (2023). Anti-synchronization of fractional-order complex-valued neural networks with a leakage delay and time-varying delays. *Chaos, Solitons & Fractals*, *174*, 113754. [CrossRef]

[35] Filippov, A. F. (2013). *Differential equations with discontinuous righthand sides: control systems* (Vol. 18). Springer Science & Business Media. [CrossRef]

[36] Zhang, G. D., & Zeng, Z. G. (2020). Stabilization of second-order memristive neural networks with mixed time delays via nonreduced order. *IEEE Transactions on Neural Networks and Learning Systems*, *31*(2), 700–706. [CrossRef]

[37] Zhang, G., & Wen, S. (2024). New approximate results of fixed-time stabilization for delayed inertial memristive neural networks. *IEEE Transactions on Circuits and Systems II: Express Briefs*, *71*(7), 3428-3432. [CrossRef]

[38] Zhang, G., & Cao, J. (2023). New results on fixed/predefined-time synchronization of delayed fuzzy inertial discontinuous neural networks: Non-reduced order approach. *Applied Mathematics and Computation*, *440*, 127671. [CrossRef]

Xiao Zhou received the B.S. degree in Mathematics and Statistics from the School of South-Central Minzu University, Wuhan, China, in 2023. She is currently pursuing the M.S. degree in applied mathematics with the School of Mathematics and Statistics, South-Central Minzu University, Wuhan, China. Her current research interests include nonlinear differential algebraic systems, neural networks, and intelligent control. (E-mail: zx187270@163.com)

Jingrui Hou received his M.S. degree in school of artificial intelligence and automation, Huazhong University of Science and Technology, Wuhan, China, in 2019. He is currently pursuing the Ph.D. degree in electrical engineering with the Royal Melbourne Institute of Technology University (RMIT), Melbourne, Australia. His current research interests include Controllability of network systems, switching systems control, multi-agent systems. (E-mail: 77567229@qq.com)

Guodong Zhang received the Ph.D. degree from the School of Automation, Huazhong University of Science and Technology, in 2014. He is currently a Professor and the Supervisor with the School of Mathematics and Statistics, South-Central Minzu University, Wuhan, China. He has published over 70 journal articles, he received the 2012 Outstanding Master's Degree Thesis Award of Hubei Province, the 2015 Outstanding Ph.D. Dissertation Award of Hubei Province, and the 2016 Chinese Association of Automation Outstanding Ph.D. Dissertation Award. And he was selected as the World Top 2% Scientists, from 2020 to 2022 and in 2024. He is an Editorial Board Member of several SCI or EI journals, such as Scientific Reports, Frontiers in Physics and Franklin Open. His current research interests include stability analysis of dynamic systems, synchronization, memristive neural networks and event-triggered control. (E-mail: zgd2008@mail.scuec.edu.cn)